Applied Physics Letters

Self-assembled nanoscale capacitor cells based on ultrathin $BiFeO_3$ films

Cite as: Appl. Phys. Lett. **104**, 182903 (2014); https://doi.org/10.1063/1.4875617
Submitted: 08 March 2014 . Accepted: 27 April 2014 . Published Online: 07 May 2014

Qing Miao, Min Zeng, Zhang Zhang, Xubing Lu, Jiyan Dai, Xingsen Gao, and Jun-Ming Liu

Self-assembled nanoscale capacitor cells based on ultrathin $BiFeO_3$ films

Qing Miao,[1] Min Zeng,[1] Zhang Zhang,[1] Xubing Lu,[1] Jiyan Dai,[2] Xingsen Gao,[1,a)] and Jun-Ming Liu[3,b)]
[1]*Institute for Advanced Materials and Laboratory of Quantum Engineering and Quantum Materials, South China Normal University, Guangzhou 510006, China*
[2]*Department of Applied Physics, The Hong Kong Polytechnic University, Hong Kong, China*
[3]*Laboratory of Solid State Microstructures, Nanjing University, Nanjing 210093, China*

(Received 8 March 2014; accepted 27 April 2014; published online 7 May 2014)

Ultrathin multiferroic $BiFeO_3$ (BFO) films with self-assembled surface nano-islands on $La_{0.67}Sr_{0.33}MnO_3$/(100) $SrTiO_3$ substrates are fabricated by a one-step pulsed laser deposition process using the Bi-rich BFO target. It is revealed that these surface nano-islands mainly consist of conductive Bi_2O_3 outgrowths, which serve as top electrodes for the nanoscale BFO capacitor cells with lateral size of 10–30 nm. The ferroelectric BFO layer underneath these Bi_2O_3 nanoislands prefers certain complex domain structure with vertical and antiparallel polarization components (the so-called "anti-domain structure") and reduced domain switching fields. Moreover, these nanoscale capacitor cells exhibit the resistive switching IV behavior, offering opportunities for application in ultrahigh density non-volatile memories. © *2014 AIP Publishing LLC*. [http://dx.doi.org/10.1063/1.4875617]

$BiFeO_3$ (BFO) has attracted intensive attentions in the past decade due to its superior magnetoelectric, photovoltaic, and electromechanical properties, in addition to its excellent ferroelectricity.[1,2] The BFO can display a large spontaneous polarization along with a canting antiferromagnetic order at room temperature,[3] making it one of the very rare room temperature single-phase multiferroics. It was also reported that the BFO thin films can exhibit extraordinarily large above-band gap photovoltages.[4,5] Moreover, in some epitaxial BFO films on $LaAlO_3$ substrate, a kind of morphotropic-like phase boundary can be stabilized, enabling a large and reversible electric-field induced strain up to 5%.[6,7] These outstanding properties make the BFO promising for a wide range of applications in high density memory, photovoltaic, electromechanical, and multiferroic devices.

With the rapid growth in demands on ultrahigh-density data storage with low power consumption, the miniaturization of ferroelectrics has become an essential issue. It is also important to understand the effects of size reduction on the physical properties of these ferroelectrics. Due to the prominent quantum size effects and highly enhanced surface-to-volume ratio, BFO nanoparticles do show some properties inaccessible otherwise.[8,9] For instance, strongly size-dependent photocatalytic and magnetic properties were observed in BFO nanoparticles.[10,11] BFO nanowires also exhibit apparent magnetic field-driven domain evolution.[12] However, up to now only a few studies focusing on the lateral size effect are available while the thickness dimension has been well addressed. The major difficulty lies in the challenges of nanoscale fabrication and characterization. Recently, strained and free standing BFO nano-islands were developed by focus ion beam (FIB) milling, and an unexpected shape memory behavior in association with a martensitic-like phase transformation was observed.[13] The FIB milling is also capable of making pre-designed BFO nanostructures with lateral size down to 170 nm, but this may not be a favored strategy for large area integration.[14] More recently, BFO nano-island arrays of ~70 nm in lateral size for each island were fabricated by pulsed laser deposition (PLD) using the thin anodic aluminum oxide (AAO) nano-templates.[15] By synthesizing such high density nano-island arrays, one may be able to fabricate memory devices of tens of Gigabit/in.[2] However, for higher density memories of Terabit/in^2, even smaller nanocapacitor cell below ~30 nm in lateral size and its arrays are required.

In this work, we report a simple one-step self-assembling method for fabricating ultra-small epitaxial BFO capacitor cells by PLD. The capacitor cells are composed of conductive bismuth-rich islands floating on the top of ultrathin BFO films (~3 nm in thickness), forming the ferroelectric capacitor cells down to ~10 nm in lateral size. These nanocapacitors can facilitate the so-call "anti-domain structures," a certain complex domain structure with antiparallel vertical polarization components. Furthermore, the nanocapacitors also exhibit polarization modulated resistive switching behaviors, enabling non-destructive read-out favored for ultrahigh density nonvolatile memory.

The BFO thin films with floating bismuth-rich islands were simply deposited using the PLD at a laser energy density of 1.0 J/cm^2 and an ambient temperature 700 °C. The core strategy here is to use a Bi-excess $Bi_{1.1}FeO_3$ target so that some Bi-rich phases or compounds can be segregated in the as-deposited thin films. In prior to the BFO film deposition, atomic flat conducting $La_{0.67}Sr_{0.33}MnO_3$ (LSMO) layer as bottom electrode was first epitaxially grown on $SrTiO_3$ (STO) substrate. By proper adjusting the deposition parameters, well defined Bi-rich islands can be easily formed. Both transmission electron microscopy (TEM) and high-resolution TEM (HRTEM) were used to obtain the cross-section images on the as-prepared samples. The ferroelectric domain structures were probed by piezoresponse force microscopy (PFM), and the

a)xingsengao@scnu.edu.cn
b)liujm@nju.edu.cn

local conductivity mapping and current-voltage (I-V) curves were obtained using conductive-AFM (Cypher, Asylum Research).

The topological, cross-section, and piezoresponse images of the as-deposited BFO thin film plus nano-islands on the LSMO/STO substrate were illustrated in Fig. 1. As shown in Fig. 1(a), rectangular-like nano-islands distributing on the BFO film surface are identified, with the lateral size of 10–30 nm and the average height of ~5 nm. These features agree well with the cross-section TEM observation shown in Fig. 1(b), which exhibits an epitaxial LSMO layer and an ultrathin BFO layer (~3 nm), along with a nanoisland on the top. The nano-island is of single crystalline nature, which has a 10:1 Bi:Fe compositional ratio, as examined by the energy-dispersive X-ray spectroscopy (EDX) probe incorporation with the HRTEM, indicating it is a bismuth-rich phase. It is worthy noting that an amorphous-like layer of ~1.0 nm in thickness appears in between the island and underneath BFO layer, which may originate from a liquid environment during the high temperature deposition and subsequent cooling process. Therefore, the island looks like to be floating on the surface of BFO film. The island is very similar to that observed previously in bismuth-rich $Bi_3Ti_4O_{12}$ by Alexe *et al.*,[16] which was suggested to be Bi_2O_3 or bismuth-rich phase precipitating from the bismuth parent phase.

To identify the phase structure, we carefully examine the HRTEM lattice refringe of the island. The details of the lattice structure and chemistry are given in the supplementary material (Figure S1).[25] The island has interplanar lattice spacings of 0.38 nm and 0.42 nm, respectively, corresponding to the (002) and (020) planes of α-Bi_2O_3 (monoclinic) with lattice constants $a = 0.59$ nm, $b = 0.83$ nm, $c = 0.75$ nm, and $\beta = 112.8°$.[17] It was reported that the α-Bi_2O_3 phase is an energetically stable phase at low temperatures, while can transform to a defect fluorite structure δ-Bi_2O_3 above ~730 °C, which is known as an excellent ionic conductor with a resistivity as low as ~1.0 Ω cm at 750 °C.[18] Although the conductivity of α-Bi_2O_3 phase is ~3 orders of magnitude lower than that of δ-Bi_2O_3, it is still much higher than that of BFO and can be considered as the nano-electrode for the underneath BFO layer. This top nano-electrode together with the bottom LSMO electrode allows the Bi_2O_3/BFO/LSMO sandwich structure to be a capacitor cell. As the lateral cell size of this island is only 10–30 nm, this capacitor should be the smallest ferroelectric BFO capacitor as far as we know, tentatively promising for Terabit/in.[2] ferroelectric based memories. Hereafter, we then focus on this type of BFO nano-capacitor cells.

First, the vertical PFM measurements were performed in order to examine the ferroelectric properties of the nano-capacitor cells. Figs. 1(c) and 1(d) show the amplitude- and phase-contrast piezoresponse micrographs for one typical sample. For the phase-contrast imaging, the bright-dark contrast usually reflects the difference in the polarization orientation (e.g., upward or downward). As shown in Fig. 1(d), the whole scanned bare area absent of any nano-island shows the uniform dark-contrast, indicating that the polarizations in this area have the similar vertical component. However, very different from this area, those small regions covered by nano-islands exhibit clear bright-contrast rather than dark one, suggesting the opposite vertical component of polarization. If looking at the details of the amplitude-contrast variation in each of these regions (Fig. 1(c)), one observes that the contrast in most of such nano-island regions is not uniform but featured with clear dark-line contrast boundary. This implies that these regions themselves are not of single-domained but rather occupied with the complex domain structure. The dark lines crossing-through these regions in the phase micrographs, as shown in Fig. 1(c), represent the domain walls. It is well known that BFO thin films may accommodate the 71°, 109°, and 180° domain boundaries. Here, we only consider the vertical component of the polarization, and use the term "anti-domain structure" for such complex domains with anti-parallel vertical polarization components (e.g., 109° or 180° domain boundaries). Such unique domain structure can be further illustrated by the combined 3D topology-piezoresponse images, shown in Figs. 1(e) and 1(f), which demonstrate the apparent "anti-domain" pattern in these regions covered by the nano-islands. This feature is very popular and of general significance in all the samples we have prepared, although for each

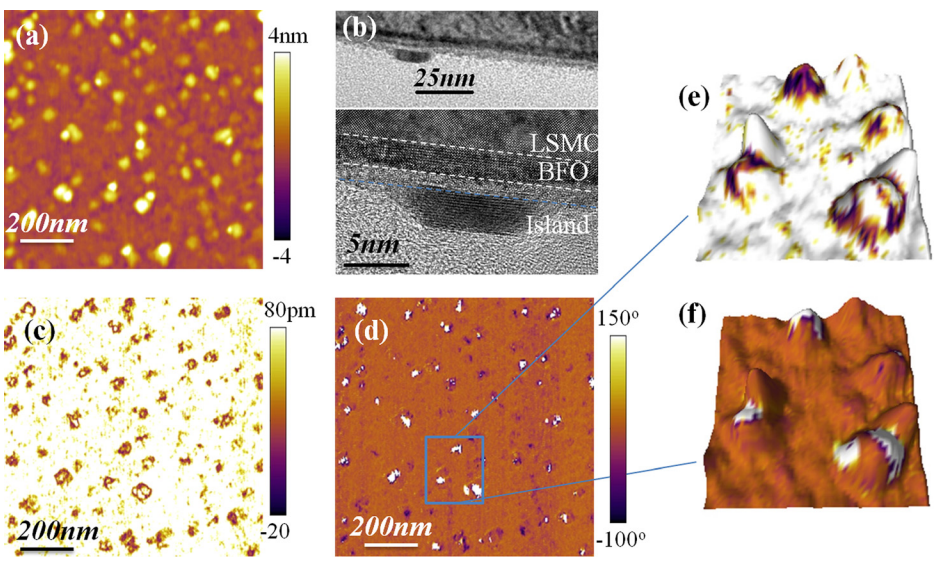

FIG. 1. AFM topography (a) and TEM image for the sample showing the self-assembled structure of nano-islands on ultrathin BFO thin film (b); piezoresponse amplitude (c) and correspondent phase images (d) for the above island-film structure; three-dimensional topographic image superimposed on its piezoresponse amplitude (e) and phase (f) mappings, based on the data from (a), (c), and (d).

case there are indeed minor island spots showing the uniform contrast. It is also worthy mentioning that the bright-contrast in the piezoelectric phase image most probably originates from the BFO layer under the islands, as the Bi_2O_3 cannot generate piezoelectric signals.

The above identified fact implies that the Bi_2O_3/BFO/LSMO sandwich cell favors the anti-domain structure in the ultrathin BFO film. This anti-domain structure may nucleate during the deposition process. One may discuss this issue from the interface build-in-voltage generated by the work function difference between the neighboring layers. In the present case, the LSMO/BFO interface creates a built-in voltage of ~0.26 V due to the work function difference, noting that the work function for LSMO is $Ø_{LSMO} = 4.96$ eV,[19] and that for BFO is $Ø_{BFO} = 4.7$ eV.[20] The built-in voltage is $V_{built} = (Ø_{LSMO} - Ø_{BFO})/e = 0.26$ V, which tends to induce the uniform polarization state in the bare BFO area (dark-contrast in Fig. 1(d)). However, for the Bi_2O_3/BFO interface, due to the big work function of Bi_2O_3 $Ø_{Bi2O3} = 6.23$ eV, a built-in voltage $V_{built} = \sim 1.5$ V with opposite orientation is generated on the top interface,[21] which competes with the V_{built} from the LSMO/BFO interface and leads to the observed anti-domains.

Given the above simple model for the Bi_2O_3/BFO/LSMO nano-capacitor cell, one can now examine the electric properties by measuring the local piezoelectric hysteresis loops. In these measurements, the conductive PFM tip was positioned at the centre of the nano-island, with the biased DC voltage varying from ±1 V to ±4 V between the PFM tip and the back LSMO electrode. The piezoresponse phase-voltage hysteresis and butterfly-like amplitude-voltage hysteresis are shown in Figs. 2(a) and 2(b), respectively. At a low bias voltage of ~1.0 V, we are not able to identify obvious phase signal change, as the bias field is far below the polarization switching field. Well-defined and saturated hysteresis loops can be obtained at a bias voltage above ~3.0 V (Fig. 2(a)), in which the asymmetric coercive fields of −1.5 V and +2.2 V can be extracted from the butterfly amplitude loop.

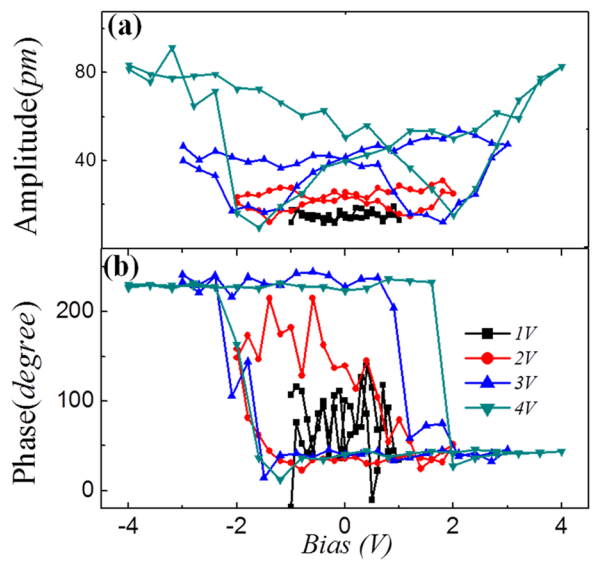

FIG. 2. PFM hysteresis loops acquired on a nano-island: piezoresponse amplitude (a) and phase (b) loops. The hysteresis loops were measured by various DC bias voltages from 1 to 4 V, respectively.

Interestingly, at a bias voltage of ~2.0 V, the polarization can be well switched in the negative bias side, while such switching is unable in the positive bias voltage side. This asymmetric behavior of the polarization switching implies strongly preferred polarization orientation (or imprint) of the domains in the nano-capacitor cell. For comparison, we also measure the voltage dependent piezoresponse on the bare area free of nano-island coverage, where the Pt AFM tip serves as the top electrode, see Figure S2 in the supplementary material.[25] It is apparent that a higher bias voltage is needed to switch the polarization of the bare area than that for switching the polarization of the nano-capacitor cells.

To gain further insight into the polarization switching of both the bare area and the nano-capacitor cells, we investigate the domain poling effect within a square range of $1.0 \times 1.0\ \mu m^2$ (Fig. 3). Prior to the switching, the original domains in this range are upward switched via the PFM tip at +2.0 V, resulting in a uniform downward polarization (not shown here). After the switching, the pattern is scanned at a bias voltage from −2.0 V to −4.0 V according to a predesigned pattern. At a bias of −2.0 V, some of the nano-island regions have been switched back to the upward polarization state, while the bare area remains unchanged, as shown in Fig. 3(a). When the bias voltage increases up to −3.0 V, most of the nano-island regions switch to the upward polarization state while only a few still remain downward (Fig. 3(b)). At an even higher voltage of −4.0 V, nearly all the pre-assigned square range is completely switched to the upward polarization state (Fig. 3(c)).

These observations indicate that the nano-islands as the top electrodes make the BFO polarization easier to switch.

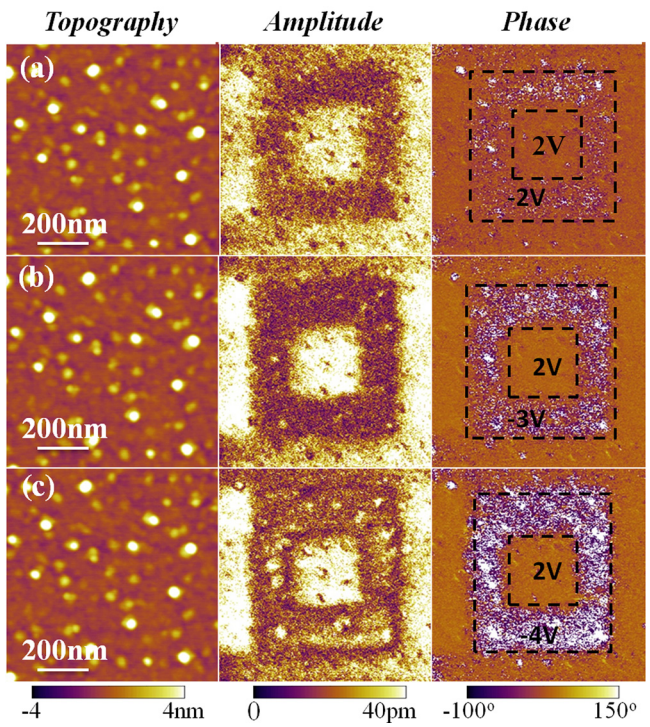

FIG. 3. The polarization switching properties for the BFO island-film structure, which shows the PFM topography, amplitude, and phase images within a square area of $1 \times 1\ \mu m^2$. Prior to the polarization switching, the initial preferred polarization patterns were first switched downward by scanning the film surface at +2 V through PFM tip. After that, the pre-pattern area is scanned upward at bias voltages of −2 V (a), −3 V (b), and −4 V (c), respectively.

Several reasons may be responsible for this effect. First, the conducting nano-islands have better electrical contact with the underneath BFO film than the AFM tip does, making the electric field more uniformly distributing inside the cell. Second, the nano-electrodes may have low interface barrier. It is noted that the nano-islands are mainly composed of Bi_2O_3, which is rather conductive and suitable to serve as nano-electrodes.[16,18]

Besides the unusual ferroelectric properties of these nano-capacitor cells, the Bi-oxide outgrowths (mainly α-Bi_2O_3) also have impact on the conductive behaviors of the BFO films, as evaluated by the conductive-AFM (CAFM). Figs. 4(a) and 4(b) show the AFM image and current mapping micrograph measured at a scanning bias of 2.0 V. The current map (Fig. 4(b)) exhibits the low-current bright-contrast background ($\sim$45 pA) and high-current dark-contrast spots (>10 nA). This is also verified by the current profile (Fig. 4(d)) taken along the straight line given in Fig. 4(b). From the current mapping, the high-current regions mostly appear on the nano-islands, indicating that the nano-electrodes can greatly enlarge the local conductivity. We also measured the current-voltage (I-V) characteristics on one nano-island, which corresponds to a high current spot (Fig. 4(c)). The measurement was carried out by sweeping the bias voltage between −3.0 V and +3.0 V. Interestingly, a well-established I-V hysteresis is clearly observed, showing an apparent resistive switching behavior with a rather big ON/OFF resistance ratio beyond 100. The resistive switching exhibits a reversible diode-like behavior. At low bias voltage, the IV curves show, respectively, forward diode and backward diode behaviors at two different polarization states, as shown in the inset of Fig. 4(c). This is similar to that reported in relatively thicker BFO films, interpreted by the modulation of interface Schottky barriers by ferroelectric polarization reversal.[22] In comparison, we observe similar resistive switching in the bare film area (see the details of the IV curves in Figure S3 in the supplementary material[25]), in which a higher bias voltage is needed to achieve similar current value. At a certain bias (e.g., 2.0 V), the observed current is much lower than that on the nano-islands, in consistent with our CAFM observation (Fig. 4(b)) and previous reports on ultrathin $BaTiO_3$ film with Ag nano-electrodes.[23]

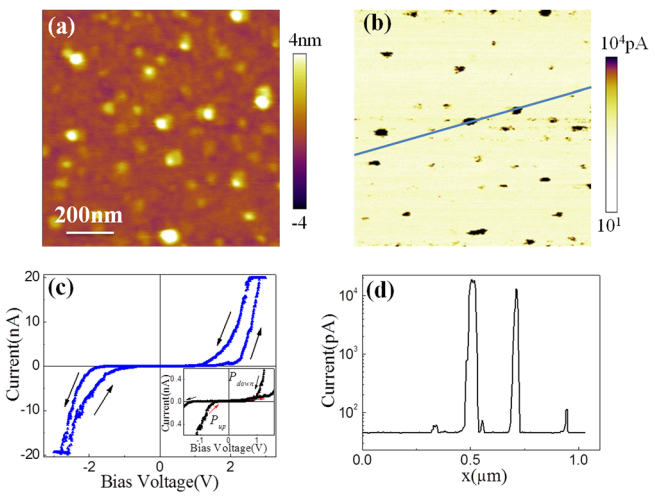

FIG. 4. AFM topological (a) and conductive-AFM current mapping (b) images for the island-BFO film structure within a square area of $1 \times 1\ \mu m^2$. A current profile along the straight line in (b) is shown in (d). IV curves on a nano-island at a bias voltage of 3 V measured at room temperature, which shows reversible diode-like resistive switching *IV* behavior (c). The inset in (c) represents the low bias voltage *IV* curves for the two opposite polarization states.

The above current mapping is similar to that observed bismuth-rich parasite phases on BFO film by Béa *et al.*, where the high current was attributed to a current shortcut between the top and bottom electrode bypassing the insulating ferroelectric layer.[24] From our observation, the nano-islands should not have direct contact with bottom electrode. Therefore, they are not shortcuts, but rather form a capacitor cell structure. To measure the local conductivity for a bare film, we usually rely on the small AFM tip as top electrode, which may form a high mechanical contact barrier, leading to a loss of effective field, and consequently to a relatively high switching field. Once a conductive Bi_2O_3 island exists, such contact barrier varnishes, resulting in the observed low switching field and an enhanced local current. Because of the polarization-modulated resistive switching, the polarization orientations can be well-reflected by the current amplitude, providing a good opportunity to construct a voltage-write current-read data storage memory. As the lateral cell size is 10–30 nm, a scaling up to Terabit/in.^{2} density for non-volatile memories become possible.

In summary, epitaxial and self-assembled BFO nano-capacitor cell structures with lateral size of 10-30 nm have been fabricated using a one-step PLD process. Each cell consists of a conductive bismuth rich nano-island as top electrode, an ultrathin BFO layer of $\sim$3.0 nm in thickness as dielectric layer, and a LSMO layer as bottom electrodes. It has been revealed that the nano-capacitor structures not only prefer to accommodate ferroelectric anti-domains in contrast to the uniform polarization state of the bare BFO area but also apparently lower the polarization switching field. The nano-capacitors also exhibit attractive resistive switching behaviors, promising for non-destructive read-out high-density (e.g., Tbit/in.^{2}) non-volatile memories.

The authors would like to thank the Natural Science Foundation of China (Grant Nos. 51031004, 51272078, and 51332007), Guangdong National Science Foundation (No. S2011040003205), the Program for International Innovation Cooperation of Guangzhou (No. 2014J4500016) National 973 Projects of China (Grant No. 2011CB922101), and the Program for Changjiang Scholars and Innovative Research Team in University of China (Grant No. IRT1243) for financial assistance.

[1]K. F. Wang, J.-M. Liu, and Z. F. Ren, Adv. Phys. **58**, 321 (2009).
[2]G. Catalan and J. F. Scott, Adv. Mater. **21**(24), 2463 (2009).
[3]J. Wang, J. Neaton, H. Zheng, V. Nagarajan, S. Ogale, B. Liu, D. Viehland, V. Vaithyanathan, D. Schlom, U. Waghmare, N. A. Spaldin, K. M. Rabe, M. Wuttig, and R. Ramesh, Science **299**(5613), 1719 (2003).
[4]S. Y. Yang, J. Seidel, S. J. Byrnes, P. Shafer, C.-H. Yang, M. D. Rossell, P. Yu, Y.-H. Chu, J. F. Scott, J. Ager III, L. W. Martin, and R. Ramesh, Nat. Nanotechnol. **5**(2), 143 (2010).
[5]A. Bhatnagar, A. R. Chaudhuri, Y. H. Kim, D. Hesse, and M. Alexe, Nat. Commun. **4**, 2835 (2013).
[6]J. X. Zhang, B. Xiang, Q. He, J. Seidel, R. J. Zeches, P. Yu, S. Y. Yang, C. H. Wang, Y.-H. Chu, L. W. Martin, A. M. Minor, and R. Ramesh, Nat. Nanotechnol. **6**(2), 98 (2011).
[7]R. Zeches, M. Rossell, J. X. Zhang, A. Hatt, Q. He, C.-H. Yang, A. Kumar, C. H. Wang, A. Melville, C. Adamo, G. Sheng, Y.-H. Chu, J. F.

Ihlefeld, R. Erni, C. Ederer, V. Gopalan, L. Q. Chen, D. G. Schlom, N. A. Spaldin, L. W. Martin, and R. Ramesh, Science **326**(5955), 977 (2009).
[8]J. H. Li, L. Chen, V. Nagarajan, R. Ramesh, and A. L. Roytburd, Appl. Phys. Lett. **84**(14), 2626 (2004).
[9]R. K. Vasudevan, K. Bogle, A. Kumar, S. Jesse, R. Magaraggia, R. Stamps, S. Ogale, H. Potdar, and V. Nagarajan, Appl. Phys. Lett. **99**(25), 252905 (2011).
[10]T.-J. Park, G. C. Papaefthymiou, A. J. Viescas, A. R. Moodenbaugh, and S. S. Wong, Nano Lett. **7**(3), 766 (2007).
[11]F. Gao, X. Y. Chen, K. B. Yin, S. Dong, Z. F. Ren, F. Yuan, T. Yu, Z. G. Zou, and J.-M. Liu, Adv. Mater. **19**(19), 2889 (2007).
[12]S. H. Xie, A. Gannepalli, Q. N. Chen, Y. M. Liu, Y. C. Zhou, R. Proksch, and J. Y. Li, Nanoscale **4**(2), 408 (2012).
[13]J. X. Zhang, X. Ke, G. Gou, J. Seidel, B. Xiang, P. Yu, W.-I. Liang, A. M. Minor, Y.-H. Chu, G. V. Tendeloo, X. B. Ren, and R. Ramesh, Nat. Commun. **4**, 2768 (2013).
[14]F. Johann, A. Morelli, and I. Vrejoiu, Appl. Phys. Lett. **99**(8), 082904 (2011).
[15]S. Hong, T. Choi, J. H. Jeon, Y. Kim, H. Lee, H.-Y. Joo, I. Hwang, J.-S. Kim, S. O. Kang, S. V. Kalinin, and B. H. Park, Adv. Mater. **25**(16), 2339 (2013).
[16]M. Alexe, J. F. Scott, C. Curran, N. D. Zakharov, D. Hesse, and A. Pignolet, Appl. Phys. Lett. **73**(11), 1592 (1998).
[17]A. Walsh, G. W. Watson, D. J. Payne, R. G. Edgel, J. H. Guo, P.-A. Glans, T. Learmonth, and K. E. Smith, Phys. Rev. B **73**, 235104 (2006).
[18]H. T. Cahen, T. G. M. Van Den Belt, J. H. W. De Wit, and G. H. J. Broers, Solid State Ionics **1**, 411–423 (1980).
[19]J. Qiu, K. J. Jin, P. Han, H. B. Lu, C. L. Hu, B. P. Wang, and G.-Z. Yang, Europhys. Lett. **79**(5), 57004 (2007).
[20]H. Yang, H. M. Luo, H. Wang, I. O. Usov, N. A. Suvorova, M. Jain, D. M. Feldmann, P. C. Dowden, R. F. DePaula, and Q. X. Jia, Appl. Phys. Lett. **92**(10), 102113 (2008).
[21]Y. Xu and M. A. A. Schoonen, Am. Mineral. **85**(3–4), 543–556 (2000).
[22]C. Wang, K. J. Jin, Z.-T. Xu, L. Wang, C. Ge, H. B. Lu, H. Z. Guo, M. He, and G.-Z. Yang, Appl. Phys. Lett. **98**, 192901 (2011).
[23]X. S. Gao, J. M. Liu, K. Au, and J. Y. Dai, Appl. Phys. Lett. **101**(14), 142905 (2012).
[24]H. Béa, M. Bibes, A. Barthélémy, K. Bouzehouane, E. Jacquet, A. Khodan, J.-P. Contour, S. Fusil, F. Wyczisk, A. Forget, D. Lebeugle, D. Colson, and M. Viret, Appl. Phys. Lett. **87**(7), 072508 (2005).
[25]See supplementary material at http://dx.doi.org/10.1063/1.4875617 for additional information on HRTEM analysis for a Bi_2O_3 nanoisland on BFO film, along with voltage dependent local piezoresponse curves on the bare film, and I-V curves for both the bare BFO film and a nanocapacitor.